Journal of Cardiothoracic Surgery

RESEARCH Open Access

YTHDF2 mediates the protective effects of MG53 on myocardial infarction injury via recognizing the m6A modification of MG53

Zhaojie Li[1*], Kai Li[2] and Jianqiang Zhao[1]

Abstract

Introduction High levels of MG53 may attenuate the damage from myocardial infarction (MI). Furthermore, N6-methyl-adenosine (m6A) methylation is a mode of RNA modification that influences mRNA functions. Whether m6A modification on MG53 exerts a protective role on myocardial injury remains largely unknown.

Materials and methods We established hypoxia/reoxygenation (H/R) H9c2 cell and myocardial ischemia reperfusion (I/R) rat models. MG53 expression was detected using RT-qPCR, and its m6A levels were measured using Me-RIP. The relationship between MG53 and YTHDF2 was evaluated using RNA immunoprecipitation, FISH and immunofluorescence assay, and luciferase reporter assay. MI area of rats was determined using TTC staining. Cell apoptosis was assessed by flow cytometry and TUNEL assay.

Results The m6A levels of MG53 were increased in H/R-induced H9c2 cells and the myocardium of I/R rats. Moreover, knockdown of YTHDF2 recognized the m6A modification of MG53 and enhanced MG53 stability. Overexpression of MG53 inhibited apoptosis of H/R-treated H9c2 cells, which was reversed by YTHDF2, while downregulation of MG53 m6A methylation caused by METTL3 knockdown further abrogated the effect induced by YTHDF2. Additionally, MG53 attenuated MI and apoptosis in I/R rats, which were rescued by YTHDF2.

Conclusion YTHDF2 hinders the protective effect of MG53 on MI by recognizing the m6A modification of MG53.

Keywords Myocardial infarction, MG53, m6A modification, YTHDF2

Introduction

Myocardial infarction (MI) is a serious coronary artery disease that subsequently leads to heart failure and sudden cardiac death, making it a leading cause of death globally [1, 2]. Despite advancements in treatment, including thrombolysis and percutaneous coronary intervention, there are currently no effective strategies available for the prevention or cure of this disease [3, 4]. The death and dysfunction of cardiomyocytes is an important pathological factor of MI [5]. Therefore, it is urgent to further explore the mechanism of cardiomyocyte death, as this knowledge may provide new targets and strategies for the clinical treatment of MI.

MG53, also called TRIM72, is a protein expressed in skeletal muscle and various other tissues that plays an essential role in the repairing of damaged plasma membranes [6]. Secreted from skeletal muscles as a muscle factor, MG53 is instrumental in the repair and generation of damaged tissues, such as muscles, heart, lungs,

*Correspondence:
Zhaojie Li
lzj737196@163.com
[1]Elderly Department, The First Affiliated Hospital of Xi'an Medical College, 48 Fenghao West Road, Lianhu District, Xi'an, Shaanxi 710077, China
[2]Clinical Medicine Department, Xi'an Medical College, No.1 Xinwang Road, Weiyang District, Xi'an, Shaanxi 710021, China

and kidneys [7, 8]. Studies have shown that mice lacking MG53 are more susceptible to diverse kinds of damage, and the application of exogenous recombinant human MG53 can alleviate damage and restore organ function [9, 10]. Recent studies have highlighted that MG53 is involved in the pathogenesis of multiple diseases, such as cancer and cardiovascular disease, positioning it as a promising therapeutic target in these diseases [11, 12]. In the context of MI, MG53 has garnered attention as an independent risk factor and a valuable prognostic biomarker [13]. Notably, MG53 levels are upregulated under ischemia/reperfusion (I/R) injury conditions and play a myocardial protective role [14]. Therefore, investigating the regulatory mechanisms of MG53 during MI will provide a theoretical foundation for elucidating its functions.

N6-methyl-adenosine (m6A) is the most common chemical modification of RNA that regulates RNA stability, splicing, translation, and exporting. This includes various types of RNA, such as mRNA, tRNA, rRNA, and non-coding RNA [15]. It is known that m6A modification affects the onset and progression of various diseases, including MI [16, 17]. The modification is reversely regulated by methyltransferases/writers and demethylases/erasers, and m6A reading proteins/readers recognize m6A-modified sites. Members of the YTH domain family (such as YTHDF1, YTHDF2, YTHDF3, YTHDC1, and YTHDC2) are m6A "readers" that recognize m6A sites to exert regulatory role in RNA processes [18]. The most important function of YTHDF2 is to promote RNA degradation [19]. A previous study has reported that YTHDF2 represses I/R-induced myocardial injury by recognizing m6A modification of BNIP3 [20]. However, it remains unclear whether YTHDF2 influences m6A modification of MG53 and how they regulate the progression of MI.

In this study, we determined the effect of YTHDF2 on the m6A modification of MG53 and the role in MI. This study may provide a new therapeutic target for the treatment of MI.

Materials and methods

Hypoxia/reoxygenation (H/R) treatment and cell transfection

Rat myocardial cell line (H9c2; RRID: CVCL_0286) was purchased from ATCC (Manassas, VA, USA). Cells were cultured with the RPMI-1640 medium (Hyclone, USA) supplemented with 10% fetal bovine serum (Gibco, USA) at 37 °C with 5% CO_2 and 95% air.

The short hairpin RNA plasmids targeting these genes (YTHDF1, YTHDF2, YTHDC1, YTHDC2, IGF2BP1, IGF2BP2, IGF2BP3, and METTL3), short hairpin RNA negative control plasmid (sh-NC), MG53 overexpression plasmids, YTHDF2 overexpression plasmids, and negative control vector were purchased from the GenePharma (Shanghai, China). The plasmids were transfected into H9c2 cells using Lipofectamine 2000 (Thermo Fisher Scientific, USA) for 48 h.

The H/R H9c2 cell model was established according to a previous study [21] with minor modifications. The cells were maintained in an incubator containing 1% O_2, 5% CO_2 and 94% N_2 for 3 h, and then incubated in 5% CO_2 and 95% air for 5 h. H9c2 cells in the control group were maintained in a normoxia environment (5% CO_2 and 95% air) for 8 h. The in vitro study design is shown in Fig. 1.

The establishment of animal model

The animal study was performed according to the Guidelines for the Care and Use of Laboratory Animals and was approved by the Ethics Committee of Xi'an Medical College.

Thirty male Sprague-Dawley rats (7 weeks old, Shanghai Institute of Animal Experimentation, Chinese Academy of Sciences) were used for the establishment of the myocardial I/R injury model. Those rats were housed in an SPF environment and randomly

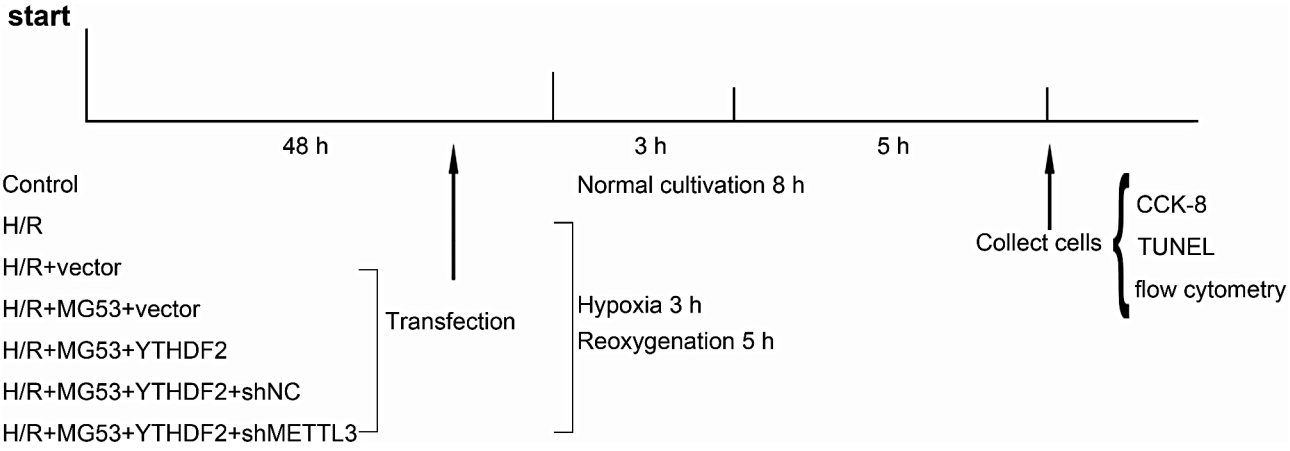

Fig. 1 The in vitro study design

divided into five groups: sham, I/R, I/R + LV (lentivirus)-NC (negative control), I/R + LV-MG53 + LV-NC, and I/R + LV-MG53 + LV-YTHDF2 groups, with six rats in each group. The I/R model was established according to a previous study [22]. Briefly, those rats were anesthetized with chloral hydrate (0.5 ml/100 g body weight). An incision was made at the fourth intercostal space. The left anterior descending (LAD) coronary artery was exposed and was ligated with a 6-0 prolene suture for 0.5 h of ischemia. Then, the artery was then released for reperfusion for 120 min. The rats of the sham group received the same surgery without the ligation. To investigate the role of MG53 and YTHDF2, LV-MG and LV-YTHDF2, as well as LV-NC were provided by GenePharma (Shanghai, China). The lentivirus (3×10^8 PFU) was injected through the tail vein two weeks before I/R model generation, once a week. Four weeks after reperfusion, all rats were killed by injecting excessive pentobarbital sodium (i.p.). The hearts were collected and immediately stored at -20 °C for 1 h followed by coronally sectioning at 1 mm. The animal study design is shown in Fig. 2.

2,3,5-triphenyltetrazolium chloride (TTC) staining

TTC staining was performed following the protocol as described previously [23]. Briefly, following the sacrifice of the rats, their myocardial tissues were sectioned into 1 mm thick slices. Next, these sections were incubated with 1% TTC staining solution for 20 min at 37℃. Then, the area of MI was analyzed using the Image-Pro Plus software.

Detection of m6A levels of MG53

The m6A levels of MG53 were measured using MeRIP according to a previous study [24]. Total RNA was extracted and purified using a commercial kit (Promega, Hong Kong). Next, the Magna methylated RNA immunoprecipitation m6A kit (Merck Millipore, Germany) was used for the immunoprecipitation of m6A-modified mRNA. Subsequently, RT-qPCR was performed to assess the enrichment of m6A-containing mRNA. Primers targeting a negative region of MG53 without m6A sites served as the negative control, while primers corresponding to the positive region of MG53 were applied as the positive control.

Luciferase reporter assays

M6A sites in MG53 were predicted using the SRAMP database. The wild-type (WT) MG53 reporter plasmids containing each specific m6A site and the mutated (MUT) MG53 reporter plasmids (Mutated at the predicted m6A site) were synthesized by Genechem company. Next, these reporter plasmids with sh-NC or sh-YTHDF2 were co-transfected into H9c2 cells with Lipofectamine 2000. The Dual-Luciferase Reporter Assay System (Promega, Madison, USA) was used to detect the luciferase activity after 48 h of transfection following the manufacturer's protocols.

RNA immunoprecipitation (RIP)

As described previously [25], RIP assay was conducted using the Magna RIP RNA-binding protein immunoprecipitation kit (Millipore, USA) following the manufacturer's protocols. Target RNA of MG53 and the negative control were deposited by the YTHDF2 antibody (ab220163, Abcam, UK, RRID: AB_2868573) and normal rabbit IgG (ab172730, Abcam, RRID: AB_2687931), respectively. Finally, RT-qPCR was employed to detect the enrichment of MG53 binding to YTHDF2.

Fluorescence in situ hybridization (FISH) and immunofluorescence assay

According to a previous study [26], H9c2 cells were seeded onto glass slide (Invitrogen, USA). After allowing the cells to adhere, they were fixed with 4% paraformaldehyde (Beyotime, China). Next, the cells were permeabilized using 0.1% Triton X-100 (Beyotime, China). The cells were incubated with a hybridization solution containing the MG53 probe at 37 ℃ overnight, followed by heat at 80 ℃ for 3 min for DNA denaturation. After washing with SCC, nonspecific binding sites were blocked with 5% bovine serum albumin (Beyotime, China). The cells were incubated with primary antibody against YTHDF2 (ab246514, Abcam, RRID: AB_2891213) at a dilution of 1:1000 at 4 ℃ overnight. After that, the cells were incubated with Alexa Fluor 488-labeled goat

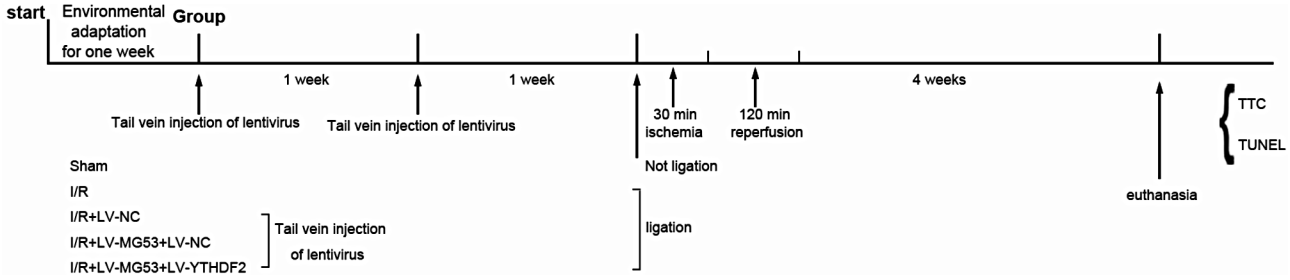

Fig. 2 The animal study design

anti-rabbit (ab150077, Abcam, RRID: AB_2630356) for 1 h in the dark room. The cells were then washed three times with PBS and treated with DAPI (Invitrogen, USA) for 3 min. Finally, the fluorescence was observed using confocal microscopy (Olympus, Japan).

CCK-8 assays

H9c2 cells were plated in 96-well plates at a density of 5×10^3 cells/100 μL per well. Then, the CCK-8 reagent (Dojindo, Japan) was diluted at a ratio of 1:10 using the culture medium, and the diluted solution was added to each well. The cells were incubated at 37 ℃ for 2 h. Finally, the absorbance was measured using a spectrophotometer (Thermo Fisher Scientific, USA).

RT-qPCR

Total RNA was extracted from H9c2 cells using TRIzol (Thermo Fisher Scientific, USA). Then, reverse transcription of RNA was performed using a commercial kit (Takara, Japan). Next, cDNA was mixed with the SYBR Green (Invitrogen, USA) and amplified using the ABI7500 system (Thermo Fisher Scientific, USA). β-actin was used as the reference gene of this assay. The relative expression of target genes was analyzed using the $2^{-\Delta\Delta Ct}$ method [27].

Western blotting

According to a previous study [28], total proteins were extracted using the RIPA buffer (Beyotime, China). The concentration of the proteins was determined using the BCA kit (Beyotime, China). The proteins were separated with 10% SDS-PAGE (Beyitime, China). Following separation, the proteins were transferred to PVDF membranes (Millipore, USA), and BSA (Beyotime, China) was used to block the membranes. Primary antibodies were diluted at a ratio of 1:1000 and incubated with the membranes for 2 h at room temperature. The primary antibodies included Bcl-2 (ab182858, Abcam, RRID: AB_2715467), Bax (ab32503, Abcam, RRID: AB_725631), cleaved caspase3 (ab2302, Abcam, RRID: AB_302962) and GAPDH (ab9485, Abcam, RRID: AB_307275). After incubation, the membranes were washed with the PBST and incubated with the corresponding secondary antibody (HRP-labeled goat anti-rabbit, ab205718, Abcam, RRID: AB_2819160) for 2 h in the dark. Finally, the bands were developed with the substrate (Millipore, USA).

Flow cytometry

Cell apoptosis was evaluated using flow cytometry as previously described [29]. H9c2 cells were digested with trypsin (Beyotime, China) and washed with PBS. Then, 5 μL Annexin V and 5 μL PI (100 μg/mL) (Beyotime, China) were incubated with the cells in the dark for 40 min. Next, the cells were washed with PBS again. Finally, flow cytometry was utilized to determine apoptosis.

TUNEL assay

As previously described [30], cardiac muscles were embedded and cut into slices. Subsequently, the tissue sections were incubated with the TUNEL staining solution (Beyotime, China) for 2 h at room temperature. Finally, the sections were observed and photographed under a fluorescence microscope (Lecia, Germany). For H9c2 cell apoptosis determination, the cells were cultured on the glass slide, fixed with 4% paraformaldehyde (Beyotime, China), and treated with 0.1% Trition X-100 (Beyotime, China) for 2 min on the ice. Next, these cells were incubated with TUNEL staining solution (Beyotime, China) for 1 h in the dark. Finally, DAPI was used to stain the cell nucleus for 3 min, and the results were observed under a fluorescence microscope.

Statistical analysis

Data in this research were analyzed using the GraphPad Prism 7.0 software. The assays were repeated three times and the data are displayed as the mean ± SD in this paper. The comparison was analyzed with one-way ANOVA. $p < 0.05$ was considered statistically significant.

Results

Aberrant m6A levels of MG53 was found in H/R-induced H9c2 cells and I/R-induced myocardial tissues

To mimic the pathological conditions of MI, we established the myocardial I/R rat model. After euthanizing the rats, we collected the myocardial tissues and measured the mRNA expression and m6A levels of MG53 using RT-qPCR and Me-RIP, respectively. The results showed that the expression of MG53 was reduced in the myocardial tissues of I/R-induced rats (Fig. 3A). Conversely, the m6A levels of MG53 were elevated in these tissues (Fig. 3B). In addition, H9c2 cells were injured after H/R stimulation. We found that the expression of MG53 was downregulated in H9c2 cells after H/R treatment (Fig. 3C), while the m6A levels of MG53 were increased in these cells (Fig. 3D). The results suggest that MG53 modified by m6A may be involved in MI progression.

YTHDF2 regulated MG53 expression by recognizing its m6A methylation

The "readers" can recognize m6A modification and affect the expression of the modified mRNA. Therefore, we chose several "readers" including YTHDF1, YTHDF2, YTHDC1, YTHDC2, IGFBP1, IGFBP2 and IGFBP3 to identify whether they affect MG53 expression. We knocked down their expression by plasmid transfection. As shown in Fig. 4A, the expression of these "readers" was decreased compared to the negative control groups,

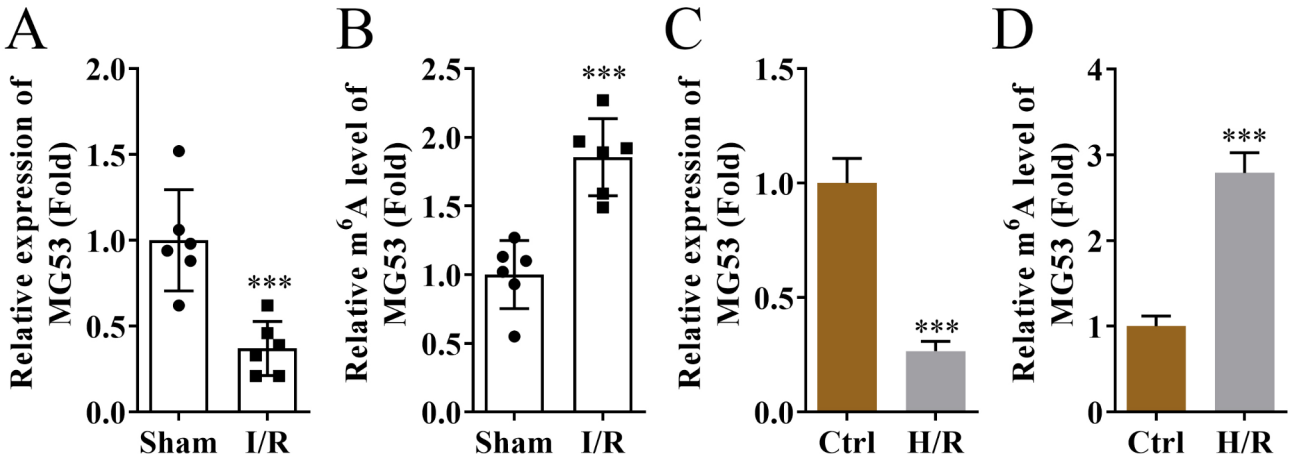

Fig. 3 Aberrant m6A levels of MG53 was found in H/R-induced H9c2 cells and I/R-induced myocardial tissues (**A**) The expression of MG53 in the myocardium of rats was determined with RT-qPCR, the results are expressed as a fold change relative to sham. $n=6$. (**B**) M6A levels of MG53 in the myocardium of rats were explored using Me-RIP, the results are expressed as a fold change relative to sham. $n=6$. (**C**) The expression of MG53 in H9c2 cells was determined with RT-qPCR, the results are expressed as a fold change relative to Ctrl. $n=3$. (**D**) The m6A levels of MG53 in H9c2 cells were determined using Me-RIP, the results are expressed as a fold change relative to control. $n=3$. ***$p<0.001$

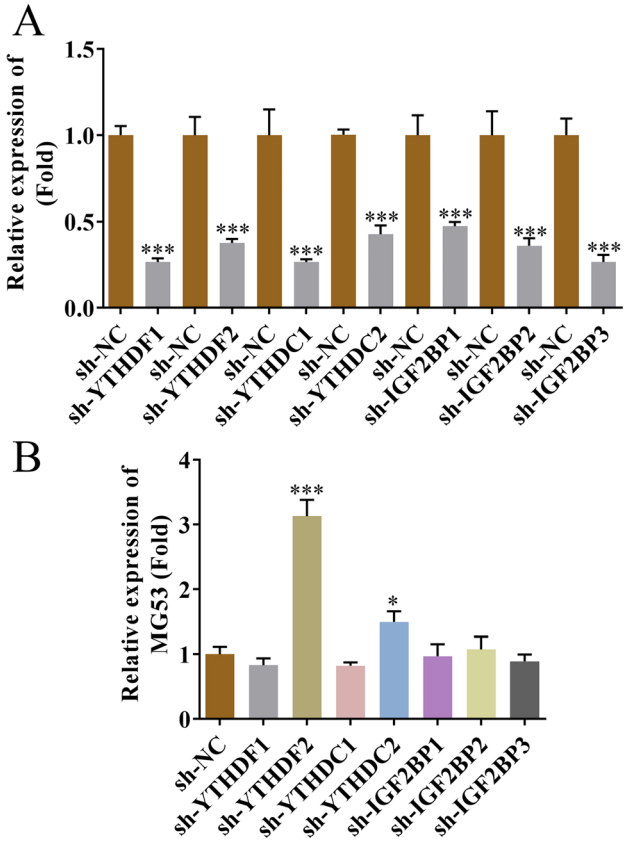

Fig. 4 The expression of MG53 was elevated after YTHDF2 knockdown in H9c2 cells (**A**) The expression of YTHDF1, YTHDF2, YTHDC1, YTHDC2, IGF2BP1, IGF2BP2 and IGF2BP3 in H9c2 cells after knockdown was determined with the RT-qPCR. (**B**) The expression of MG53 in H9c2 cells after knocking down YTHDF1, YTHDF2, YTHDC1, YTHDC2, IGF2BP1, IGF2BP2 and IGF2BP3 was explored with RT-qPCR. The results are expressed as a fold change relative to sh-NC. $n=3$. *$p<0.05$, ***$p<0.001$

suggesting successful transfection. Then, the results of RT-qPCR revealed that the levels of MG53 were dramatically increasing after YTHDF2 knockdown in H9c2 cells (Fig. 4B). Thus, we chose YTHDF2 for further study.

RIP assay results indicated that the enrichment of MG53 RNA was increased in the YTHDF2 group (Fig. 5A), suggesting that YTHDF2 interacts with MG53. Five potential m6A sites were predicted in MG53 (Fig. 5B). The two sites with high confidence were chosen, and the luciferase reporter assay was performed to confirm the modifying sites. Results showed that the luciferase activity was enhanced in the site 2 WT group following YTHDF2 knockdown, but was not changed in the site 1 WT group (Fig. 5C and D), suggesting that site 2 in MG53 is the m6A site. Then, MG53 stability was evaluated, and the results showed that the stability of MG53 was increased in the YTHDF2 knockdown group (Fig. 5E). Moreover, immunofluorescence and FISH assays were performed for further verification of the location of MG53 and YTHDF2 in H9c2 cells. As shown in Fig. 5F, the YTHDF2 protein co-localized with MG53 RNA in H9c2 cells. Taken together, knockdown of YTHDF2 stabilizes MG53 mRNA by recognizing m6A modification of MG53, which increases MG53 expression in H9c2 cells.

The YTHDF2/MG53 axis regulates apoptosis of H9c2 cells in a m6A-dependent manner

To evaluate the effect of MG53 and YTHDF2 on the apoptosis of H9c2 cells, we established the MG53 and YTHDF2 overexpressed H9c2 cells. Results of RT-qPCR showed that the levels of MG53 and YTHDF2 in the overexpression group were higher than that in the vector group (Fig. 6A and B). We found that YTHDF2 did

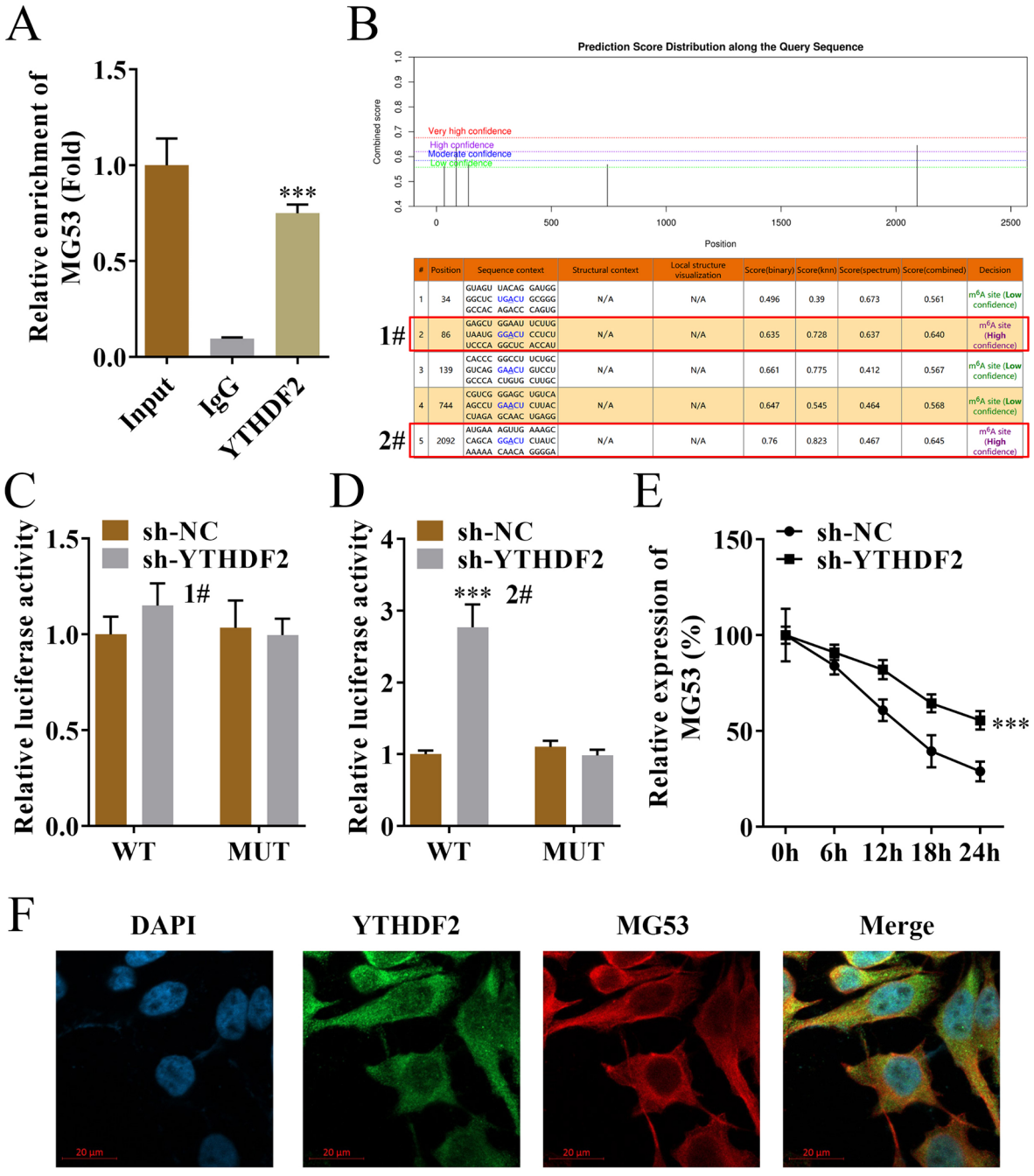

Fig. 5 YTHDF2 directly regulated MG53 in rat myocardial cells (**A**) The binding between YTHDF2 and MG53 mRNA was determined with RNA immunoprecipitation. (**B**) Potential m6A sites in MG53 were predicted using the SRAMP database. (**C, D**) Luciferase reporter gene assay was performed to detect the binding relationship between YTHDF2 and MG53 to identify the m6A sites in MG53. (**E**) The stability of MG53 in H9c2 cells after YTHDF2 knockdown was detected with RT-qPCR. (**D**) The co-localization of MG53 and YTHDF2 in H9c2 cells was determined with immunofluorescence and RNA FISH. $n = 3$. ***$p < 0.001$

not regulate m6A levels of MG53 (Fig. 6C). To investigate whether MG53 m6A methylation is involved in cardiomyocyte apoptosis, we used METTL3 to regulate MG53 m6A modification. After shMETTL3 transfection, METTL3 expression was reduced (Fig. 6D), MG53 m6A levels were upregulated (Fig. 6E), and then MG53 expression was also increased (Fig. 6F). Cell phenotypes were analyzed using CCK-8, TUNEL, and flow cytometry. H9c2 cell viability was suppressed after the stimulation of H/R. Overexpression of MG53 promoted the viability of H/R-induced cells, which was reversed by YTHDF2 overexpression. However, METTL3 knockdown further

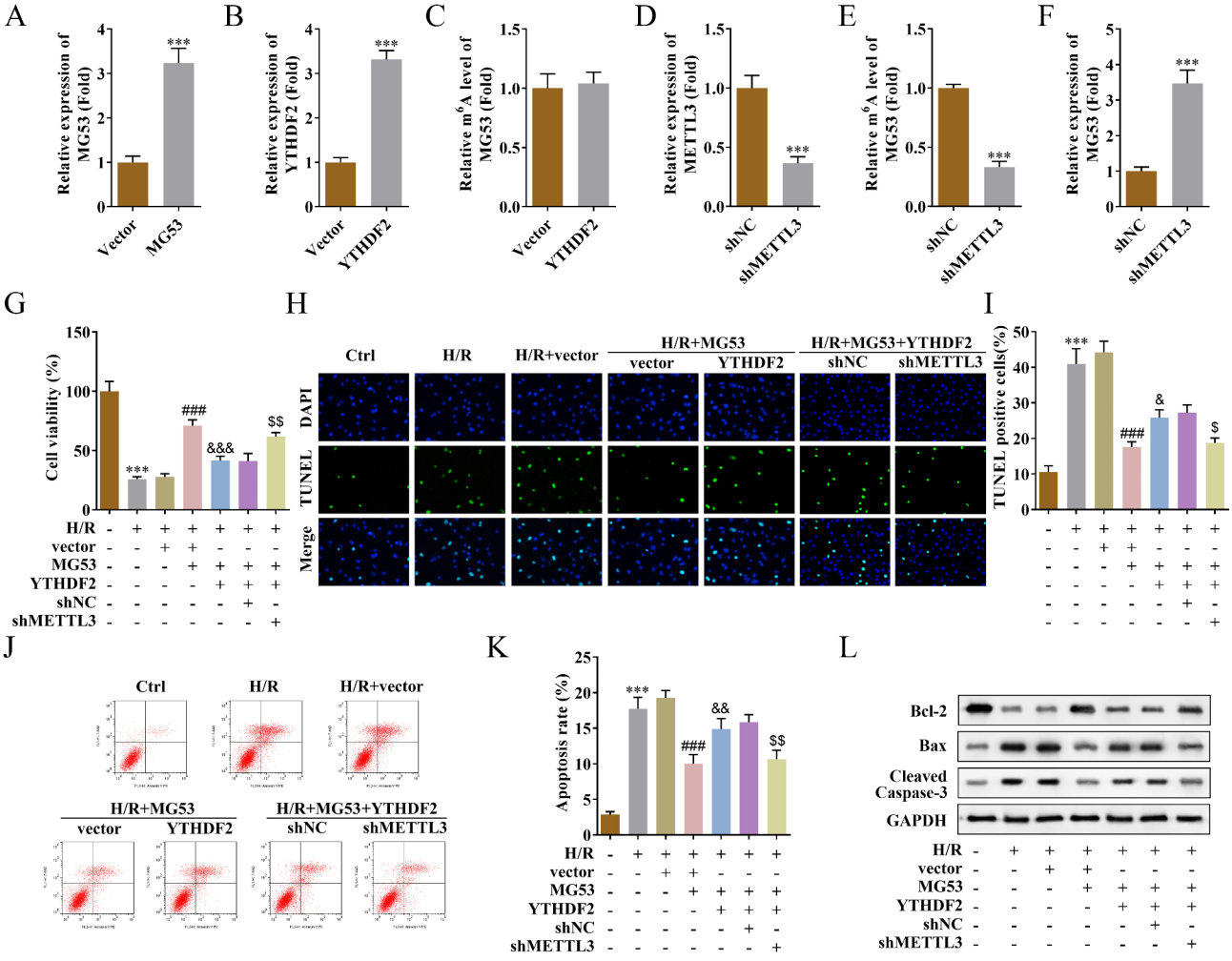

Fig. 6 The YTHDF2/MG53 axis regulates apoptosis of H9c2 cells in a m6A-dependent manner (**A**, **B**) The expression of MG53 and YTHDF2 in H9c2 cells was determined using RT-qPCR, the results are expressed as a fold change relative to vector. (**C**) The effect of YTHDF2 on m6A levels of MG53 was measured using Me-RIP, the results are expressed as a fold change relative to vector. (**D**) The expression of METTL3 in H9c2 cells was measured using the RT-qPCR, the results are expressed as a fold change relative to shNC. (**E**) The effect of METTL3 knockdown on m6A levels of MG53 was measured using Me-RIP, the results are expressed as a fold change relative to shNC. (**F**) The effect of METTL3 knockdown on MG53 expression was measured using RT-qPCR, the results are expressed as a fold change relative to shNC. (**G**) The viability of H9c2 cells was detected with CCK-8 assays. (**H, I**) The apoptosis of H9c2 cells was evaluated using TUNEL staining. (**J, K**) Flow cytometry was performed to determine apoptosis of H9c2 cells. (**H**) The levels of apoptosis-related proteins in H9c2 cells were detected by western blotting. $n = 3$. ***$p < 0.001$. ###$p < 0.001$.&&&$p < 0.001$. && and \$\$$p < 0.01$. & and \$ $p < 0.05$

rescued the effect of YTHDF2 on cell viability (Fig. 6G). Conversely, as shown in Fig. 6H and K, H/R treatment aggravated apoptosis of H9c2 cells. Overexpression of MG53 inhibited apoptosis of these cells, while YTHDF2 abrogated this inhibition, which was further reversed by METTL3 knockdown. Finally, the levels of apoptosis-related proteins were determined with western blotting. We found that H/R increased Bax and cleaved caspase-3 protein levels but reduced Bcl-2 levels in H9c2 cells. Overexpression of MG53 partly recovered the levels of Bcl-2 and inhibited the expression of Bax and cleaved caspase-3, which was rescued by YTHDF2. However, METTL3 knockdown abrogated the effects of YTHDF2 on the levels of these apoptosis-related proteins (Fig. 6L). Together, YTHDF2 reversed the inhibition of cardiomyocyte apoptosis caused by MG53, which depended on the m6A modification of MG53.

YTHDF2 accelerates the MI progression of rats by regulating MG53

In this part, we explored the role of YTHDF2 and MG53 in vivo. TTC staining was performed to determine the MI area of rats in each group. Results revealed that overexpression of MG53 reduced MI area in I/R-induced rats, whereas overexpression of YTHDF2 reversed the effect caused by MG53 (Fig. 7A and B). Subsequently, TUNEL staining was conducted to analyze apoptosis in the myocardium. The images showed that overexpression

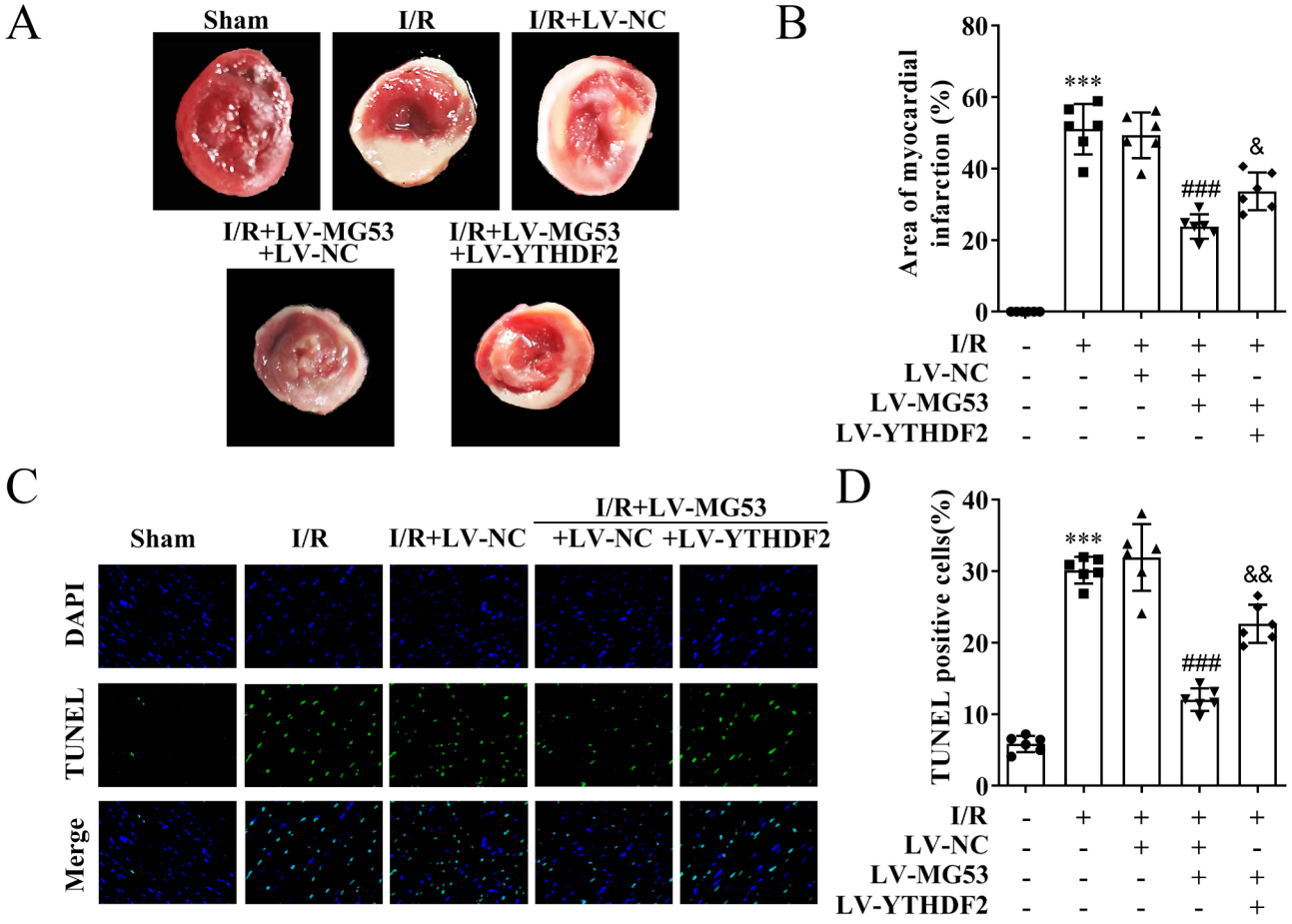

Fig. 7 YTHDF2 accelerates MI progression of rats by regulating MG53 (**A, B**) The MI area was detected using TTC staining. (**C, D**) TUNEL staining was performed to determine apoptosis in the myocardium of rats. $n=6$. ***$p<0.001$. ###$p<0.001$. &&$p<0.01$. &$p<0.05$

of MG53 suppressed apoptosis of cardiomyocytes in rats, while overexpression of TYHDF2 abrogated the effects induced by MG53 (Fig. 7C and D).

Discussion

Myocardial cell apoptosis triggered by ischemia and hypoxia is a primary cause of MI [31]. Thus, investigating the regulatory mechanisms of myocardial cell apoptosis may provide theoretical support for developing a new treatment for MI. In this research, we elucidated the effect of YTHDF2 on m6A-modified MG53 during the development of MI.

MG53 is expressed primarily in the heart. Thus, several previous studies have identified its role in heart diseases. Accumulating evidence has demonstrated that MG53 has a potential cardioprotective effect [32]. A recent study has found that MG53 has a dual role in the heart; while it can protect the heart, persistently high levels of MG53 may trigger insulin resistance and cardiovascular complications [33]. Hence, it is of great significance to investigate the role of MG53 in MI. Several studies have investigated its role in myocardial I/R injury and its regulatory mechanism. For example, MG53 could maintain the integrity of mitochondria in myocardial cells, thereby alleviating myocardial I/R injury [34]. In addition, MG53 inhibits necroptosis caused by myocardial I/R injury by degradation of RIPK1 [35]. Wang et al. [36] have performed in vitro experiments and found that MG53 suppresses inflammation response and apoptosis of cardiomyocytes. In our study, we found that the expression of MG53 was decreased in H/R-induced H9c2 cells and I/R-induced rats. Moreover, overexpression of MG53 inhibited myocardial apoptosis both in vitro and in vivo, as well as reduced MI area in rats, suggesting MG53 protects the heart from damage and decelerates MI progression. Our findings are consistent with previous evidence that MG53 has a protective effect against I/R-induced injury [37]. However, we have not assessed whether the levels of MG53 undergo dynamic changes during the I/R process. It remains uncertain whether MG53 is expressed at elevated levels under I/R and H/R conditions, and whether high levels of MG53 further promote myocardial injury. In future studies, we will measure the expression levels of MG53 and explore its role

in cardiomyocyte apoptosis at different I/R and H/R time points.

M6A methylation is the most common post-transcriptional modification of RNA that is closely related to cardiovascular diseases. A previous study has demonstrated that inhibition of MG53 m6A methylation can suppress apoptosis and oxidative stress of cardiomyocytes, thereby attenuating MI [14]. This study suggests that the m6A modification of MG53 plays an important role in the progression of MI. Therefore, we measured the m6A levels of MG53 and investigated the regulatory mechanisms. We found that the m6A levels of MG53 were enhanced in the myocardium of I/R rats and H/R-treated H9c2 cells, suggesting that m6A-modified MG53 is involved in MI. We focused on investigating m6A "readers" in our study, who could specifically recognize the target m6A-modified mRNA and play a role in the modulation of RNA processing, degradation, translocation and translation [18, 38]. Our study results showed that YTHDF2 interacted with MG53 and affected MG53 expression; however, its did not regulate m6A methylation of MG53. Moreover, YTHDF2 affects mRNA degradation [19]. Thus, we measured MG53 stability and found that YTHDF2 knockdown enhanced MG53 stability. YTHDF2 plays a critical role in the development of heart diseases, such as diabetic cardiomyopathy and cardiac hypertrophy [39, 40]. Cai et al. [20] have found that YTHDF2 relieves myocardial I/R-induced injury. Conversely, Xu et al. [41] have reported that inhibition of YTHDF2 attenuates myocardial I/R-induced damage. These studies suggest that YTHDF2 plays a double-edged role in I/R-induced injury. In this study, we identified that overexpression of YTHDF2 reversed the inhibition of cardiomyocyte apoptosis and MI induced by MG53, suggesting that YTHDF2 aggravates MI. Based on the contradictory results of previous studies, we hypothesized that YTHDF2 may also dynamically change at different I/R or H/R time points, which will be further explored in our subsequent studies. Additionally, we knocked down METTL3 to reduce the m6A levels of MG53 and found cell apoptosis was inhibited, indicating that the effect of MG53 on myocardial injury depends on its m6A modification, further demonstrating that YTHDF2 promotes MI by recognizing m6A methylation of MG53.

Limitations exist in this study. The recovery of myocardial contractility of rats after MG53 and YTHDF2 overexpression was not evaluated. Moreover, the upstream factors that can affect the functions caused by YTHDF2 need to be further explored. Additionally, whether YTHDF2/m6A/MG53 axis affects the behaviors of other types of cells, such as fibroblasts and endothelial cells, remains not understood. Importantly, translating the results of this study into clinical applications will be the goal of our future research. We initially plan to study the effect of YTHDF2 and MG53 on MI in more advanced animal models and test the expression levels of YTHDF2 and MG53, and the m6A level of MG53 in a large number of human patient samples to verify our findings, which will provide a more reliable basis for clinical research.

In conclusion, we delved deeper into the mechanisms underpinning the development of MI. We demonstrate that YTHDF2 promotes cardiomyocyte apoptosis by recognizing the m6A methylation of MG53, thereby exacerbating MI. These findings provide new promising targets for the clinical treatment of MI.

Supplementary Information

The online version contains supplementary material available at https://doi.org/10.1186/s13019-024-03210-y.

Supplementary Material 1

Acknowledgements

Not applicable.

Author contributions

ZL conceived the study; ZL conducted the experiments; LK and JZ analyzed the data; ZL was a major contributor in writing the manuscript. All authors read and approved the final manuscript.

Funding

This study was supported by Key R&D Projects in Shaanxi Province (2023-YBSF-599).

Data availability

The datasets used and/or analyzed during the current study are available from the corresponding author on reasonable request.

Declarations

Ethics approval and consent to participate

The study was approved by the Ethics Committee of Xi'an Medical College (XYLS2022221). All experiments were performed in accordance with relevant guidelines and regulations.

Competing interests

The authors declare no competing interests.

Received: 24 July 2024 / Accepted: 24 December 2024
Published online: 08 February 2025

References

1. Barrere-Lemaire S, Vincent A, Jorgensen C, Piot C, Nargeot J, Djouad F. Mesenchymal stromal cells for improvement of cardiac function following acute myocardial infarction: a matter of timing. Physiol Rev. 2024;104(2):659–725.
2. Sun Q, Ma H, Zhang J, You B, Gong X, Zhou X, et al. A self-sustaining antioxidant strategy for effective treatment of myocardial infarction. Adv Sci (Weinh). 2023;10(5):e2204999.
3. Zhang Z, Sheng Z, Che W, An S, Sun D, Zhai Z, et al. Design and rationale of the ATTRACTIVE trial: a randomised trial of intrAThrombus Thrombolysis versus aspiRAtion thrombeCTomy during prImary percutaneous coronary interVEntion in ST-segment elevation myocardial infarction patients with high thrombus burden. BMJ Open. 2023;13(11):e76476.
4. Schafer A, Konig T, Bauersachs J, Akin M. Novel therapeutic strategies to reduce reperfusion Injury after Acute myocardial infarction. Curr Probl Cardiol. 2022;47(12):101398.

5. Qi B, Song L, Hu L, Guo D, Ren G, Peng T, et al. Cardiac-specific overexpression of Ndufs1 ameliorates cardiac dysfunction after myocardial infarction by alleviating mitochondrial dysfunction and apoptosis. Exp Mol Med. 2022;54(7):946–60.
6. Cai C, Masumiya H, Weisleder N, Matsuda N, Nishi M, Hwang M, et al. MG53 nucleates assembly of cell membrane repair machinery. Nat Cell Biol. 2009;11(1):56–64.
7. Bian Z, Wang Q, Zhou X, Tan T, Park KH, Kramer HF, et al. Sustained elevation of MG53 in the bloodstream increases tissue regenerative capacity without compromising metabolic function. Nat Commun. 2019;10(1):4659.
8. Wang YF, An ZY, Li JW, Dong ZK, Jin WL. MG53/TRIM72: multi-organ repair protein and beyond. Front Physiol. 2024;15:1377025.
9. Jia Y, Chen K, Lin P, Lieber G, Nishi M, Yan R, et al. Treatment of acute lung injury by targeting MG53-mediated cell membrane repair. Nat Commun. 2014;5:4387.
10. Zhang Y, Lv F, Jin L, Peng W, Song R, Ma J, et al. MG53 participates in ischaemic postconditioning through the RISK signalling pathway. Cardiovasc Res. 2011;91(1):108–15.
11. Du Y, Li T, Yi M. Is MG53 a potential therapeutic target for cancer? Front Endocrinol (Lausanne). 2023;14:1295349.
12. Liu SM, Zhao Q, Li WJ, Zhao JQ. Advances in the study of MG53 in Cardiovascular Disease. Int J Gen Med. 2023;16:6073–82.
13. Xie H, Yan Z, Feng S, Zhu T, Zhu Z, Ni J, et al. Prognostic value of circulating MG53 levels in Acute myocardial infarction. Front Cardiovasc Med. 2020;7:596107.
14. Li D, Li L, Dong S, Yu Y, Zhang L, Jiang S. Alkylation Repair Homolog 5 regulates N(6)-methyladenosine (m6A) methylation of Mitsugumin 53 to attenuate myocardial infarction by inhibiting apoptosis and oxidative stress. J Cardiovasc Pharmacol. 2024;83(2):183–92.
15. Fu Y, Dominissini D, Rechavi G, He C. Gene expression regulation mediated through reversible m(6)a RNA methylation. Nat Rev Genet. 2014;15(5):293–306.
16. Zhang H, Shi X, Huang T, Zhao X, Chen W, Gu N, et al. Dynamic landscape and evolution of m6A methylation in human. Nucleic Acids Res. 2020;48(11):6251–64.
17. Gong R, Wang X, Li H, Liu S, Jiang Z, Zhao Y, et al. Loss of m(6)a methyltransferase METTL3 promotes heart regeneration and repair after myocardial injury. Pharmacol Res. 2021;174:105845.
18. Jiang X, Liu B, Nie Z, Duan L, Xiong Q, Jin Z, et al. The role of m6A modification in the biological functions and diseases. Signal Transduct Target Ther. 2021;6(1):74.
19. Wang L, Dou X, Chen S, Yu X, Huang X, Zhang L, et al. YTHDF2 inhibition potentiates radiotherapy antitumor efficacy. Cancer Cell. 2023;41(7):1294–308.
20. Cai X, Zou P, Hong L, Chen Y, Zhan Y, Liu Y, et al. RNA methylation reading protein YTHDF2 relieves myocardial ischemia-reperfusion injury by downregulating BNIP3 via m(6)a modification. Hum Cell. 2023;36(6):1948–64.
21. Wang Z, Yao M, Jiang L, Wang L, Yang Y, Wang Q, et al. Dexmedetomidine attenuates myocardial ischemia/reperfusion-induced ferroptosis via AMPK/GSK-3beta/Nrf2 axis. Biomed Pharmacother. 2022;154:113572.
22. Zhang Y, Liu D, Hu H, Zhang P, Xie R, Cui W. HIF-1alpha/BNIP3 signaling pathway-induced-autophagy plays protective role during myocardial ischemia-reperfusion injury. Biomed Pharmacother. 2019;120:109464.
23. Niu X, Zhang J, Ni J, Wang R, Zhang W, Sun S et al. Network pharmacology-based identification of major component of Angelica Sinensis and its action mechanism for the treatment of acute myocardial infarction. Biosci Rep, 2018,38(6).
24. Zhou Z, Cao Y, Yang Y, Wang S, Chen F. METTL3-mediated m(6)a modification of lnc KCNQ1OT1 promotes doxorubicin resistance in breast cancer by regulating miR-103a-3p/MDR1 axis. Epigenetics. 2023;18(1):2217033.
25. Wang X, Tian L, Li Y, Wang J, Yan B, Yang L, et al. RBM15 facilitates laryngeal squamous cell carcinoma progression by regulating TMBIM6 stability through IGF2BP3 dependent. J Exp Clin Cancer Res. 2021;40(1):80.
26. Zhang M, Liu R, Wang F. Telomere and G-Quadruplex colocalization analysis by immunofluorescence fluorescence in situ hybridization (IF-FISH). Methods Mol Biol. 2019;1999:327–33.
27. Zucha D, Kubista M, Valihrach L. Tutorial: guidelines for single-cell RT-qPCR. Cells, 2021,10(10).
28. Wen Z, Mai Z, Zhu X, Wu T, Chen Y, Geng D, et al. Mesenchymal stem cell-derived exosomes ameliorate cardiomyocyte apoptosis in hypoxic conditions through microRNA144 by targeting the PTEN/AKT pathway. Stem Cell Res Ther. 2020;11(1):36.
29. Liu L, Yan M, Yang R, Qin X, Chen L, Li L, et al. Adiponectin attenuates lipopolysaccharide-induced apoptosis by regulating the Cx43/PI3K/AKT pathway. Front Pharmacol. 2021;12:644225.
30. Liu Y, Xing J, Li Y, Luo Q, Su Z, Zhang X et al. Chronic hypoxia-induced cirbp hypermethylation attenuates hypothermic cardioprotection via down-regulation of ubiquinone biosynthesis. Sci Transl Med, 2019,11(489).
31. Frangogiannis NG. Pathophysiology of myocardial infarction. Compr Physiol. 2015;5(4):1841–75.
32. Zhong W, Benissan-Messan DZ, Ma J, Cai C, Lee P. Cardiac effects and clinical applications of MG53. Cell Biosci. 2021;11(1):115.
33. Jiang W, Liu M, Gu C, Ma H. The pivotal role of Mitsugumin 53 in Cardiovascular diseases. Cardiovasc Toxicol. 2021;21(1):2–11.
34. Gumpper-Fedus K, Park KH, Ma H, Zhou X, Bian Z, Krishnamurthy K, et al. MG53 preserves mitochondrial integrity of cardiomyocytes during ischemia reperfusion-induced oxidative stress. Redox Biol. 2022;54:102357.
35. Wang Q, Park KH, Geng B, Chen P, Yang C, Jiang Q, et al. MG53 inhibits necroptosis through ubiquitination-dependent RIPK1 degradation for Cardiac Protection following Ischemia/Reperfusion Injury. Front Cardiovasc Med. 2022;9:868632.
36. Wang Y, Zhou H, Wu J, Ye S. MG53 alleviates hypoxia/reoxygenation-induced cardiomyocyte injury by succinylation and ubiquitination modification. Clin Exp Hypertens. 2023;45(1):2271196.
37. Xu B, Wang C, Chen H, Zhang L, Gong L, Zhong L, et al. Protective role of MG53 against ischemia/reperfusion injury on multiple organs: a narrative review. Front Physiol. 2022;13:1018971.
38. Zhao Y, Shi Y, Shen H, Xie W. M(6)A-binding proteins: the emerging crucial performers in epigenetics. J Hematol Oncol. 2020;13(1):35.
39. Shao Y, Li M, Yu Q, Gong M, Wang Y, Yang X, et al. CircRNA CDR1as promotes cardiomyocyte apoptosis through activating hippo signaling pathway in diabetic cardiomyopathy. Eur J Pharmacol. 2022;922:174915.
40. Kmietczyk V, Oelschlager J, Gupta P, Varma E, Hartl S, Furkel J, et al. Ythdf2 regulates cardiac remodeling through its mRNA target transcripts. J Mol Cell Cardiol. 2023;181:57–66.
41. Xu GE, Yu P, Hu Y, Wan W, Shen K, Cui X, et al. Exercise training decreases lactylation and prevents myocardial ischemia-reperfusion injury by inhibiting YTHDF2. Basic Res Cardiol. 2024;119(4):651–71.

Publisher's note